



Prediction of vulnerability map regarding to the dynamic parameters and land use changes

Amirreza Sepehrara¹ · Saman Javadi² · Abbas Hosseini¹ · Neamat Karimi³

Received: 4 August 2022 / Accepted: 13 August 2023 / Published online: 30 September 2023
© The Author(s), under exclusive licence to Springer-Verlag GmbH Germany, part of Springer Nature 2023

Abstract

Quality management and developing monitoring programs to prevent further contamination of aquifers are among the essential goals of preparing groundwater vulnerability maps. Therefore, if a reliable vulnerability map can be prepared for the coming years, the quality management of aquifers will be facilitated. Recently, the land use layer has been embedded in the DRASTIC model as an influential layer, where its changes are very noticeable in the future. In this study, for the first time, groundwater vulnerability maps were obtained considering the land use prediction (Lu_{pre}) layer under a new model called DRASTIC- Lu_{pre} for the years 2030, 2040, and 2050. Since some DRASTIC variables such as recharge and groundwater level are dynamic and change over time, their maps were extracted from the MODFLOW code after model recalibration and validation. Moreover, the land change package in TerrSet software was used to predict land use in the coming years. Finally, the vulnerability map was predicted for three periods by combining the future land use maps and considering the DRASTIC dynamic variables resulting from the MODFLOW. The results showed that the regions with high and very high vulnerability values are very different in terms of area and scattering in 2040 and 2050 compared to the current situation. So that the areas with very high vulnerability values will increase by 14% and 50% in 2040 and 2050, respectively, compared to 2020. Therefore, quality management and monitoring of aquifers can be conducted with higher performance using vulnerability maps in the coming years.

Keywords Land use prediction · Vulnerability · Remote sensing · TerrSet · MODFLOW

Introduction

Aquifers are one of the essential sources of drinking water supply, especially in arid and semi-arid regions, including Iran (Javadi et al. 2011; Nadiri et al. 2022; Voutchkova et al. 2021). In recent decades, the vulnerability of groundwater resources has increased dramatically due to the increasing demand for water in the drinking, industrial, and agricultural sectors, climate changes, and human activities (Yu et al. 2022; Zhang et al. 2018). Therefore, it is necessary to provide conservation management solutions to preserve

these valuable resources (Sahoo et al. 2016). Preparing vulnerability maps can be the most optimal and economical solution in this field (Kardan Moghaddam et al. 2016). The concept of groundwater vulnerability was first proposed by Margat: the ease of reaching contamination to the groundwater resources (Nadiri et al. 2017). Various methods have been proposed to evaluate groundwater vulnerability. Provided by the United States Environmental Protection Agency (US-EPA), The DRASTIC model is the most common and widely used method due to the number of essential and available variables (Aller et al. 1987). The DRASTIC method has been used for many aquifers worldwide in the last decade to assess vulnerability (Neshat et al. 2014; Allouche 2016; Javadi et al. 2017; Neshat and Pradhan 2017; Machiwal et al. 2018; Salem et al. 2019; Kumar and Krishna 2020; Maghrebi et al. 2020, 2021; Nahin et al. 2020; Balaji et al. 2021; Noori et al. 2021).

Although the high application of this method, it only considers the nature of the aquifer and not the human factor. In this regard, for the first time, to consider human activities,

✉ Saman Javadi
javadis@ut.ac.ir

¹ Department of Civil Engineering, Science and Research Branch, Islamic Azad University, Tehran, Iran

² Department of Water Engineering, College of Agriculture Technology, University of Tehran, Tehran, Iran

³ Department of Water Resources Study and Research, Water Research Institute, Tehran, Iran

Secunda et al. (1998) added the land use layer to this model and evaluated the groundwater vulnerability using the DRASTIC model integrated with agricultural land use. They reported promising results using the integrated model. Al-Adamat et al. (2003) obtained the risk and vulnerability map for a basaltic aquifer using geographic information system (GIS), remote sensing (RS), and DRASTIC. They did not use the hydraulic conductivity data in the DRASTIC model due to some missing data and instead used the land use map as an additional factor to prepare the risk potential map. Hao et al. (2017) showed that by adding aquifer thickness (M), groundwater exploitation (E), and land use (L), the modified DRMSICEL method provided better results than the standard DRASTIC method. Asadi et al. (2017) used DRASTIC-Lu by adding the land use layer in their studies, and the results were better than DRASTIC.

In all DRASTIC and even DRASTIC-Lu studies available in the literature, the vulnerability map is prepared only for the existing situation. In other words, the effect of land use changes, such as the conversion of forests to agricultural lands or the change of barren lands to urban areas, has not been considered. Many researchers have stated that land use change, along with climate change, has significant effects on intensifying floods and reducing groundwater recharge (Mango et al. 2011). Some even believe that land use change has a more significant impact than climate change on aquifer recharge reduction (Aggarwal et al. 2012). In addition, the weak planning for land use has caused forests and pastures to be destroyed or turned into agricultural lands, resulting in less water penetration upstream and faster water flow toward the plains (Purandara et al. 2018).

Urbanization in land-use map and anthropogenic distribution could be the origin of the emission of pollutants that constitutes a serious health risk in urban areas. The main process is urbanization that may lead to waterproofing of land surface in urban areas, depending on land-use changes. This may have effect on groundwater recharge process; consequently, groundwater quality may be impact by changes in overlaying land use, i.e., industrial development, agricultural activity and wastewater generation. Industrial and agricultural impacts depend of industrial and economic development of the city (Porcel et al. 2014; Niedertscheider et al. 2014).

Therefore, since aquifer restoration is very costly and time-consuming after its pollution, the most appropriate way is to predict and identify areas prone to pollution, followed by implementing prevention measures. Thus, it is helpful to prepare a vulnerability prediction map, called DRASTIC-Lu_{pre}, to monitor and manage the quality of groundwater tables in the future. Since some variables of DRASTIC-Lu such as soil, saturated and unsaturated area, and topography are relatively constant over time, only groundwater level, recharge, hydraulic conductivity, and land use should be

predicted to use DRASTIC-Lu_{pre}. In this study, for the first time, the effects of land use changes in the next 30 years have been studied on the vulnerability of an aquifer in Iran. In addition, due to the dynamic nature of some variables of DRASTIC, the MODFLOW model has also been used to predict groundwater level and aquifer recharge.

Materials and methods

Study area

Hashtgerd Plain (50°29′–51°6′ E, 35°47′–36°7′ N) is located in the central part of Iran with an area of 411 km² (Fig. 1). The climate of the region in the northern parts is semi-humid and gradually tends to be semi-arid toward the southern parts with a decrease in altitude. The average annual temperature of the plain is 14 °C, and its long-term average rainfall is 270 mm. Most of the water consumption in the plain is for drinking, industry, and agriculture sectors, provided from groundwater resources. The dominant agricultural products in the area include wheat, barley, corn, and alfalfa. In addition, the representative hydrograph of the plain aquifer shows that during the last few decades, the groundwater level has decreased by an average of 0.65 m per year. Exploratory excavations and geoelectrical studies conducted in Hashtgerd Plain have estimated the thickness of the aquifer to be between 100 and 300 m. The maximum thickness is located in the middle parts, and it decreases with increasing the distance from the middle parts (Groundwater Budget Report 2018).

According to the geological and hydrogeological data, the plain slope decreases from the north to the south, and the direction of the surface water and groundwater flow is from the northeast to the southwest. The coarse-grained sediments in the north of the plain, especially the alluvial cone of the Kordan River, have created a suitable place for aquifer recharge from surface flows. By traveling from the northern parts of the plain to the south, the sediments become finer, and the depth of the aquifer decreases. The most considerable depth of coarse-grained sediments can be observed in the alluvial cone of the Kordan River, where the highest depth of the aquifer is in this part. In the western and southwestern regions of the plain, the depth of sediments decreases. In addition, in the southern half of the plain, a multi-layered and pressurized aquifer is observed, where the exploitation wells yield less than the northern and eastern parts due to the finer-grained sediments compared to the northern half.

Methodology and data collection

According to Fig. 2, the methodology of this study included four main parts: (a) the vulnerability map was calculated

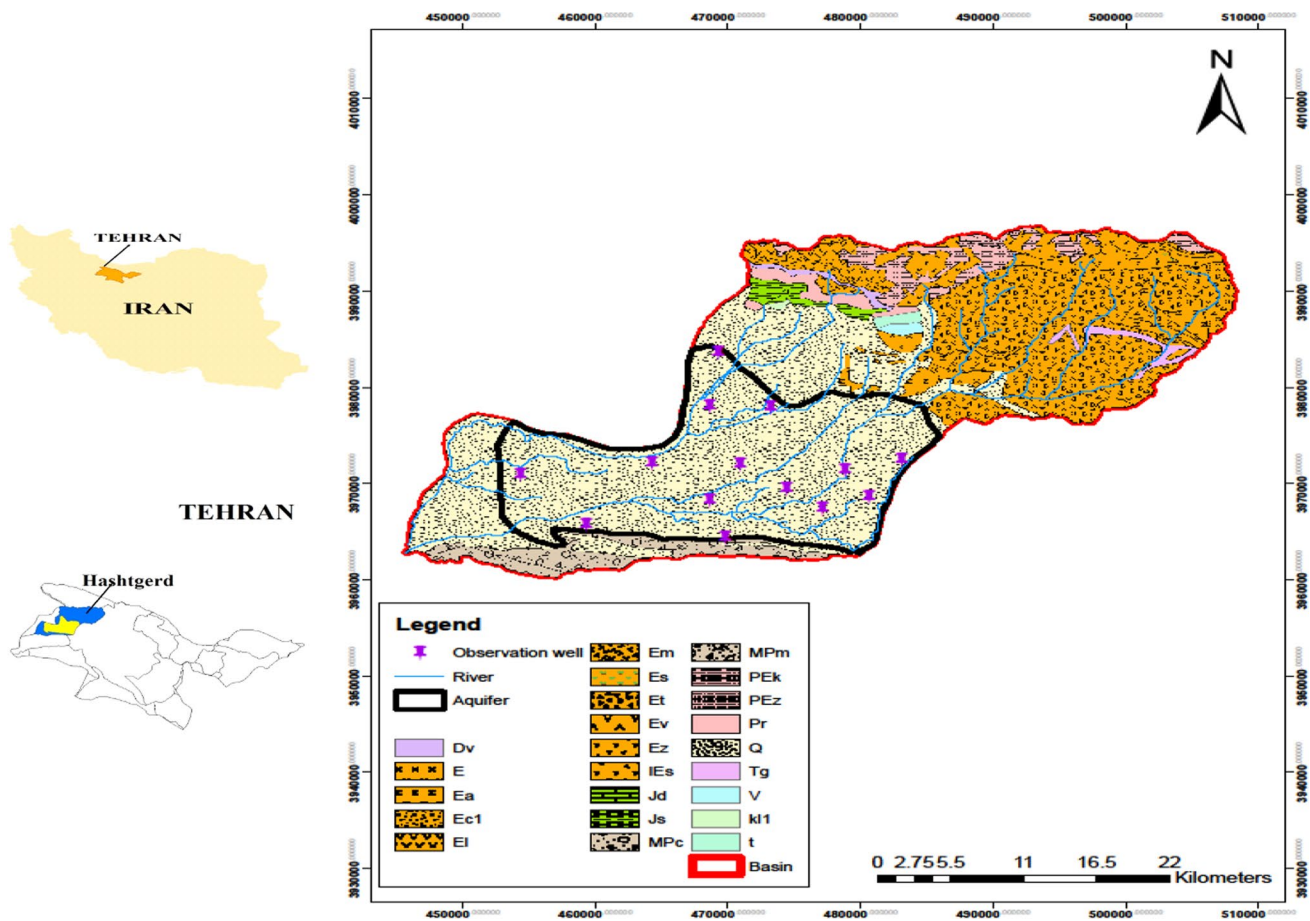


Fig. 1 Location of the Hashtgerd plain, along with the Geology map and aquifer boundary

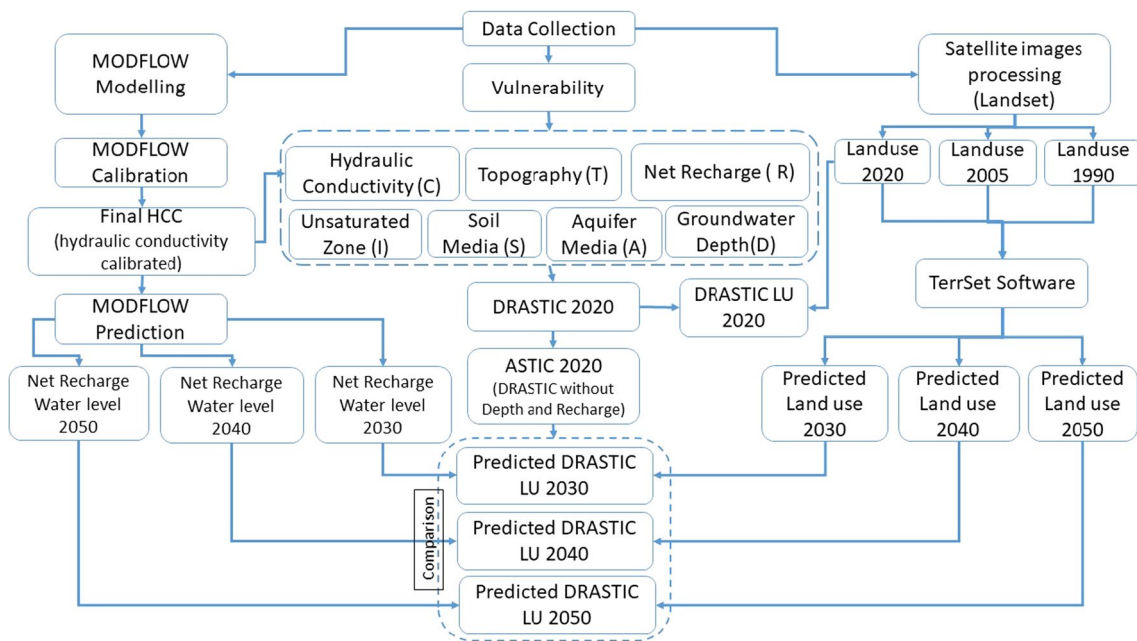


Fig. 2 Flow diagram visualizing the input data for DRASTIC, groundwater flow model, and land use maps

using the DRASTIC method, followed by extracting the DRASTIC-Lu map in the current status (2020) by considering the land use layer; (b) future land use changes were predicted for 2030, 2040, and 2050 using the TerrSet software and training available satellite images; (c) the simulation of groundwater flow for a 2-year period (2018–2020) was calibrated and validated using the MODFLOW code and GMS (Groundwater Modelling System) software; (d) finally, by combining the obtained future land use maps, and changes in groundwater level, recharge, and hydraulic conductivity calibrated (HCC), DRASTIC-Lu_{pre} vulnerability map was determined for the three periods of 2030, 2040, and 2050.

The summary of the data used in this study and their sources is presented in Table 1. All the available data on the Hashtgerd plain in various formats was integrated in a geodatabase using ArcGIS 10.1. The inputs consisted of hydrological, hydrogeological, and sample measurements of the plain. The hydrogeological data, such as the water table, soil, vadose and aquifer media, were interpolated by the Kriging interpolation technique. Other parameters, such as DEM, hydraulic conductivity, and water balance, were collected directly from the Water Organization of Alborz.

DRASTIC and DRASTIC-Lu methods

DRASTIC method

The most common method for assessing aquifer vulnerability based on the potential of groundwater contamination is the DRASTIC method, proposed by the National Groundwater Association (NGWA) in collaboration with US-EPA (Aller et al. 1987). According to the importance of model variables on pollution transmission, each variable is given a weight between one and five, where five is the most important and one is the least important. The DRASTIC method determines the aquifer vulnerability to pollution using seven hydrological, hydrogeological, geological, and topographical variables: groundwater depth (*D*), recharge (*R*), aquifer media (*A*), soil media (*S*), topography (*T*), the impact of vadose zone (*I*), and hydraulic

conductivity (*C*). Each variable is rated based on a raster map with a numerical value between 1 and 10 (Almasri 2008). Finally, the vulnerability index for each point of the study area is calculated as a weighted sum of the rating of seven variables (Eq. 1):

$$VI = D_R \times D_W + R_R R_W + A_R A_W + S_R S_W + T_R T_W + I_R I_W + C_R C_W \quad (1)$$

where VI indicates the DRASTIC vulnerability index and the W and R indices indicate the weight and rating for each variable, respectively. The main limitation of this model is in determining the relative values of rating and weight (Saidi et al. 2011). According to Eq. (1), vulnerability assessment using the DRASTIC method requires relatively less data than other models and can be evaluated with various hydrogeological parameters (Wang et al. 2012). Table 2 shows the relative weight of each variable. DRASTIC vulnerability index proposed by Aller et al. (1987) is one of the most common and well-known methods in determining vulnerability of alluvial aquifers. In addition, parameters are gained weights varying from 1 to 5 regarding their contributions to groundwater vulnerability (Aller et al. 1987). The weights in DRASTIC index is a tool for expressing the relative importance of the parameters in controlling groundwater vulnerability.

According to the conditions of the region and the characteristics of the aquifer, a rating is assigned to each of the DRASTIC variables based on Aller et al. (1987).

Table 2 Weighting of DRASTIC variables (Aller et al. 1987)

DRASTIC variables	Weight
Groundwater depth (<i>D</i>)	5
Recharge (<i>R</i>)	4
Aquifer media (<i>A</i>)	3
Soil media (<i>S</i>)	2
Topography (<i>T</i>)	1
Impact of vadose zone (<i>I</i>)	5
Hydraulic conductivity (<i>C</i>)	3

Table 1 Data used for the preparation of the vulnerability map

Data type/Parameters	Source	Date	Model of processing	Frequency/resolution
Groundwater table/observation wells	Water Organization of Alborz	2018–2020	Interpolation	Monthly/point
Geology map/Aquifer and Vadose map	Geological Survey of Iran	2010	Collected	Decade/100 × 100 m
Exploration Log/Soil map	Soil and Water Research Institute of Alborz	2015	Collected	Decade/100 × 100 m
Hydrogeological Data/Transmissivity	Water Organization of Alborz	2015	Interpolation	Decade/100 × 100 m
Geological profiles/Aquifer thickness	Water Organization of Alborz	2015	Interpolation	Decade/100 × 100 m
Water balance/recharge map	Water Organization of Alborz	2019–2020	Calculated	Annually/Lump
Satellite images/Land use maps	Landsat data	1990–2005–2020	Supervised classification	Annually/1000 × 1000

DRASTIC-Lu method

By predicting future land use, it is possible to investigate the changes in the vulnerability of aquifers. In the DRASTIC-Lu method, the land use map is added as a parameter (Lu) to the DRASTIC vulnerability method (Eq. 2):

$$\text{DRASTIC} - \text{Lu} = \text{VI} + \text{Lu}_R \times \text{LU}_W \quad (2)$$

where VI indicates the DRASTIC vulnerability index and W and R indices indicate the weight and rating for the land use variable, respectively. The land use layer is prepared according to the urban use map, the agricultural use map, as well as the coverage of the area, and it is divided into four classes: residential, agricultural, pasture, and barren. The rating of each class of land use is given in Table 3. In addition, the weight of the land use layer is five, according to previous studies (Secunda et al. 1998).

Land use changes assessment

Land use maps classification

To predict land use changes, it was necessary to extract land use maps of different periods using satellite images. Therefore, land use maps were prepared using the data of ETM+ (Enhanced Thematic Mapper Plus), TM (Thematic Mapper), and OLI (The Operational Land Imager) sensors of Landsat satellite and the ENVI 5.3 software. Satellite images have a vital role to play in the preparation of maps of land use and their changes, especially in regions with a large vegetation cover. In this study, approximately 15–20 days were elapsed between satellite images. A cloudy satellite image, however, would greatly reduce the quality of the images, thereby reducing the number or quality of images recorded by the satellite. As a result, receiving images in a short period of time is the key to receiving images without clouds. At each point in time, satellite images of the growing season (May and June) were analyzed. The satellite data included the images of Landsat 5 TM sensor in 1990, Landsat 7 ETM+ sensor in 2005, and Landsat 8 OLI sensor in 2020.

To be ensured that the satellite data were free of any radiometric, banding, and geometric errors (Birhanu et al. 2019),

geometric and radiometric corrections were performed on the images in the ENVI software. After examining the existing land uses in the area, land uses were extracted in the form of four classes: residential, agricultural, pastures, and barren. Then, samples were taken from satellite images for each of the defined classes. 70% of the collected samples were used for training, while the rest for validation. According to Tarawally et al. (2019), samples were randomly collected from satellite images using visual interpretation and with the help of topographic maps and images from Google Earth. Then, the land use maps of 1990, 2005, and 2020 were prepared using the maximum likelihood algorithm as a reliable and widely used supervised classification method in the ENVI software. This algorithm evaluates the variance and covariance of classes (Islam 2018). After preparing land use maps, the results were validated using 30% of the collected samples. Kappa coefficient was used to evaluate the generated maps and classification accuracy. Kappa coefficients for land use maps of 1990, 2005, and 2020 were 87%, 89%, and 92%, respectively. The results indicated that the highest Kappa coefficient belonged to the year 2020, possibly due to the stronger radiometric resolution of the images. The land use map for 2020 is depicted in Fig. 3a.

Prediction of future land use changes

The LCM land change package was used in the TerrSet software to predict land use maps in the coming years. This software uses the Markov cellular automata (CA-Markov) to predict land use changes. CA-Markov mode is one of the commonly used models among many LULC modeling tools and techniques, which model both spatial and temporal changes (Regmi et al. 2014; Weng 2002). The advantages of this model is often used in monitoring, ecological modeling, simulation changes, trends of the LULC and to predict the amount of land use change and the stability of future land development in the area of interest. In addition, this model is widely used to characterize the dynamics of LULC, forest cover, urban sprawl, plant growth, and modeling of watershed management (Subedi et al. 2013; Weng 2002). CA-Markov model combines cellular automata and Markov chain to predict the LULCC trends and characteristics over time. Moreover, the CA-Markov model is one of the planning support tools for the analysis of temporal changes and spatial distribution of LULC (Hua 2017). It is also important to land use policy design and planning and objectives of sustainable land use development (Ghosh et al. 2017).

First, the land use maps related to the first and last periods, including the years 1990, 2005, and 2020 were entered into the software, and then, using these maps, the changes during the period of 1990–2005 were revealed and analyzed. Variables that were effective on land use changes, such as maps of the distance from residential areas, distance from

Table 3 Land use ratings (Secunda et al. 1998)

Land use category	Ratings
Agricultural area	8
Forest	1
Pasture area	5
Open area	1
Build Up area	10

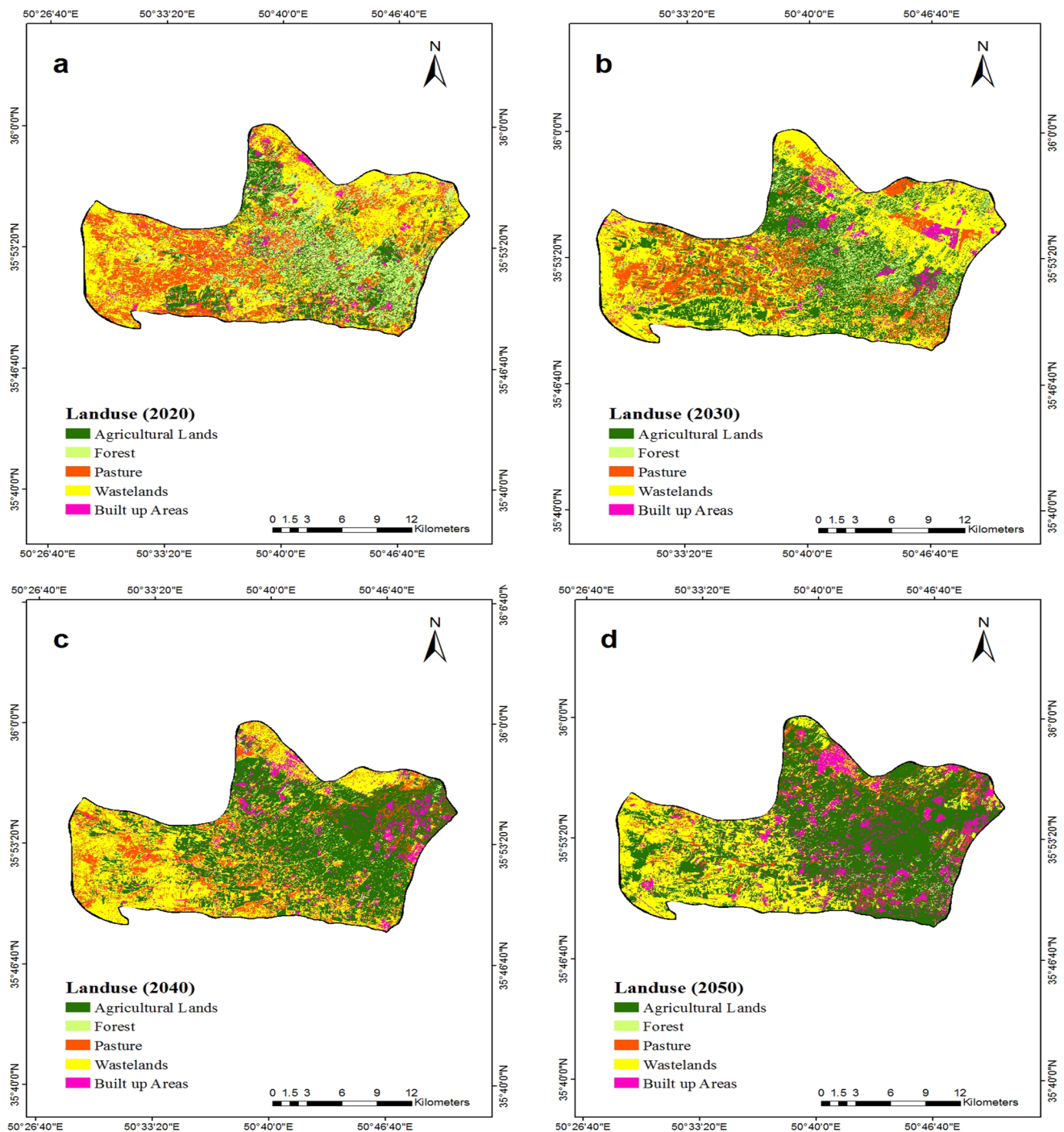


Fig. 3 Land use maps of current and future status (2020, 2030, 2040, and 2050)

the river, land slope, direction, and topographic maps, were also entered into the software as input. Based on the input data, the conversion potential of each use to other uses was calculated in TerrSet software. In other words, the probability of changing the use of each pixel to other uses in the future was calculated. Many variables affecting the change, such as height, slope, and direction, were constant during

the period, so they were static, and some others, such as distance from the river and distance from residential areas, were dynamic. Artificial neural networks (ANNs) were used to predict the conversion potential in this study. ANN is capable of grouping the potential of converting a set of uses into other uses in a set of sub-models or even modeling and calculating the potential of converting all uses into other

uses in a single sub-model. Finally, after adjusting the sub-models, the land use map of 2020 was predicted using the Markov chain method in the TerrSet software.

The performance of TerrSet software was evaluated using the error matrix method during the validation stage. To assess the performance of TerrSet, kappa coefficients were used as indices. Equation (3) is provided for estimating the Kappa coefficient, which is commonly used as an indicator of inter-rater reliability, in which P_a is proportion of trails in which judges agree and P_c is proportion of trails in which agreement would be expected due to chance:

$$Kappa = \frac{(P_a - P_c)}{(1 - P_c)} \times 100 \quad (3)$$

Kappa coefficients range from zero to 1, where a kappa coefficient of 1 indicates a completely correct classification, a value of zero indicates randomness, and a value of negative indicates a classification error.

After taking samples from satellite images for each defined class, they were divided into training (70% of the images) and test (30%) sets for validation. With the aid of ENVI software, land use maps for 1990, 2005, and 2020 were prepared using a supervised classification method utilizing the maximum likelihood algorithm. Using 30% of the collected samples and the Kappa coefficient, the results of the land use mapping were evaluated and validated. The Kappa coefficient for the prepared land use maps of 1990, 2005, and 2020 were 87.23%, 89.12%, and 92.13%, respectively. Based on the 0.92 Kappa coefficient for the validation stage, the model represents acceptable performance for 2020. Land-use maps for 2050 were predicted after the model was validated. A land use map for 2050 has been produced after validation of the model with a possible and reasonable percentage, based on which the DRASTIC changes of the study area have been estimated over the next 30 years.

After the model validation, the land use maps of 2030, 2040, and 2050 were predicted (Fig. 3b–d). The results showed that in 2050, compared to 2020, pasture areas decreased by 91%, agricultural areas increased by 300%, residential areas increased by 8 times, and barren areas decreased by 8 times.

Groundwater modeling

Some variables of the DRASTIC method, such as groundwater level and recharge, are dynamic with respect to time and will significantly change land use. Therefore, in this study, groundwater modeling system (GMS 10.4.1) software was used to extract recharge and groundwater level maps of the future.

A conceptual and numerical model of the aquifer was constructed using the MODFLOW code. Based on the

continuity equation and the finite-difference method, this numerical model is based on the partial differential equation (Eq. 4) with a constant density:

$$\frac{\partial}{\partial x} \left[k_x \frac{\partial h}{\partial x} \right] + \frac{\partial}{\partial y} \left[k_y \frac{\partial h}{\partial y} \right] + \frac{\partial}{\partial z} \left[k_z \frac{\partial h}{\partial z} \right] = S_y \pm W \quad (4)$$

where K is the hydraulic conductivity along the X , Y , and Z axes, h is the hydraulic head, W represents the aquifer's recharge with a positive sign or its discharge with a negative sign, S_y the aquifer specific yield and t time. Hashtgerd plain was considered heterogeneous and isotropic in this study, and its aquifer was considered free.

Considering the 411 km² area of the alluvial aquifer, 500 × 500 m² cells were utilized during the simulation. According to the balance report of the region, the inflow capacity to the aquifer was considered 93.6 MCM, while the outflow from the aquifer was 11.7 MCM (Fig. 4). The inlets and outlets within the Hashtgerd aquifer were determined by considering surface water flows, flood channels, rivers, streams, and snowfall at upstream heights.

An estimation of groundwater recharge was performed using the M-WetSpas distribution model. Using physical and experimental relationships, M-WetSpas simulates the annual or seasonal average of groundwater recharge. Having created raster maps in the ArcGIS software, all inputs are stored in the model as raster maps. An output map of the model is also included, as well as a file summarized the basin averaging. Input raster maps to the model are land use map, soil texture map, groundwater depth map (unsaturated root zone), rainfall map, temperature map, irrigation map, wind speed map, pan evaporation map, and Leaf area index map. (Abdollahi et al. 2017).

Groundwater evaporation occurs in areas, where the depth of the water table is less than 5 m. Accordingly, in groundwater simulations, evaporation was considered in such areas in this study. Water is exploited from 3697 wells throughout the region, most of which are located in the central and northern parts of the aquifer. The water table was estimated based on data collected from 16 observation wells and was calibrated for both steady- and unsteady-state conditions.

Model calibration for the steady and unsteady states

Using the GMS software, trial and error calibrations were conducted in steady and unsteady states. In October 2018, the steady-state groundwater model was calibrated for hydraulic conductivity based on the slightest fluctuations in groundwater levels. Furthermore, during the calibration process, the results obtained in a steady state were used to analyze the monthly unsteady state data for November 2018 to September 2020. In the unsteady state, the storage coefficient was also calibrated. In steady-state conditions, model

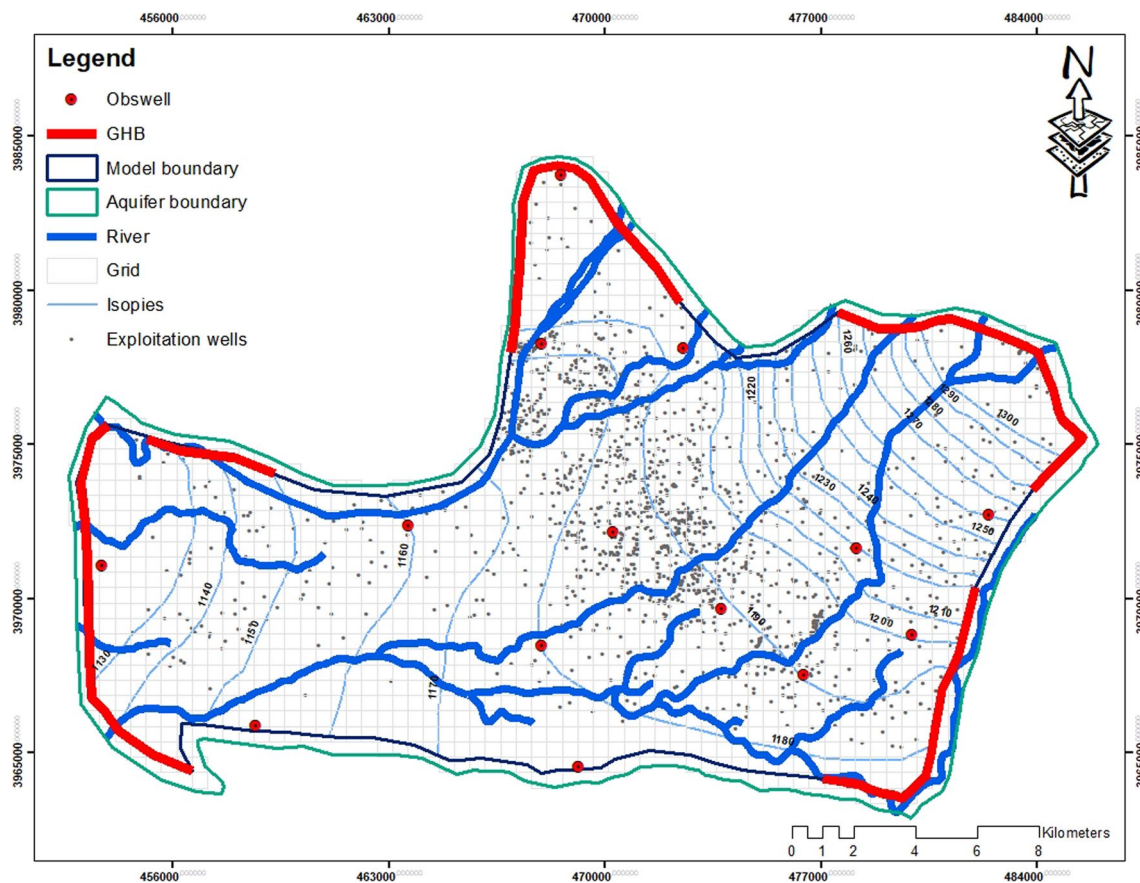


Fig. 4 Aquifer boundaries and observation well locations around the Hashtgerd aquifer

calibration was based on initial hydraulic conductivity (initial HC). Using GIS software, the initial hydraulic conductivity was calculated on the basis of the transmissivity map divided by the thickness of the aquifer ($HC = T/b$). At the end of the process, the final hydraulic conductivity (final HC) will be calibrated. At the end of the process, the final hydraulic conductivity (final HC) will be calibrated.

Following calibration for 2018 to 2020, the model was evaluated using coefficient of determination (R^2) root mean square error (RMSE) and mean absolute error (MAE). Calibration of the groundwater level in steady and unsteady states showed the largest difference between observed and calculated values at 1/5 m.

In the quantity modeling period, the simulation error is based on differences between the observed and simulated measurements of below 50 cm. The model error is in total less than 1%. Table 4 presents the final model error values in steady and unsteady stages for Hashtgerd aquifer. It appears that during the calibration phase, the coefficient of determination (R^2) is acceptable with more than 95%. This model shows good performance at steady state with RMSE and MAE values of 0.56 and 0.26, respectively. In the calibration step for the unsteady state, these values were estimated

Table 4 Flow model errors under steady and un-steady states meters

Error parameters	Steady model	Unsteady model
R^2	0.98	0.96
Mean Abs. Error	0.26	0.68
RMSE-Error	0.56	0.83

at 0.83 and 0.68, respectively. The values in Table 4 relate to the final model's error values under steady and unstable conditions.

Results and discussion

DRASTIC and DRASTIC-Lu maps in the current status

In this section, the vulnerability map in the current status is determined by extracting the map of each of the seven variables of DRASTIC. Then, the DRASTIC-Lu map for 2020 is obtained by adding the classified land use map.

The map of groundwater depth (Fig. 5a) was obtained by the statistics of the measured groundwater level. The map

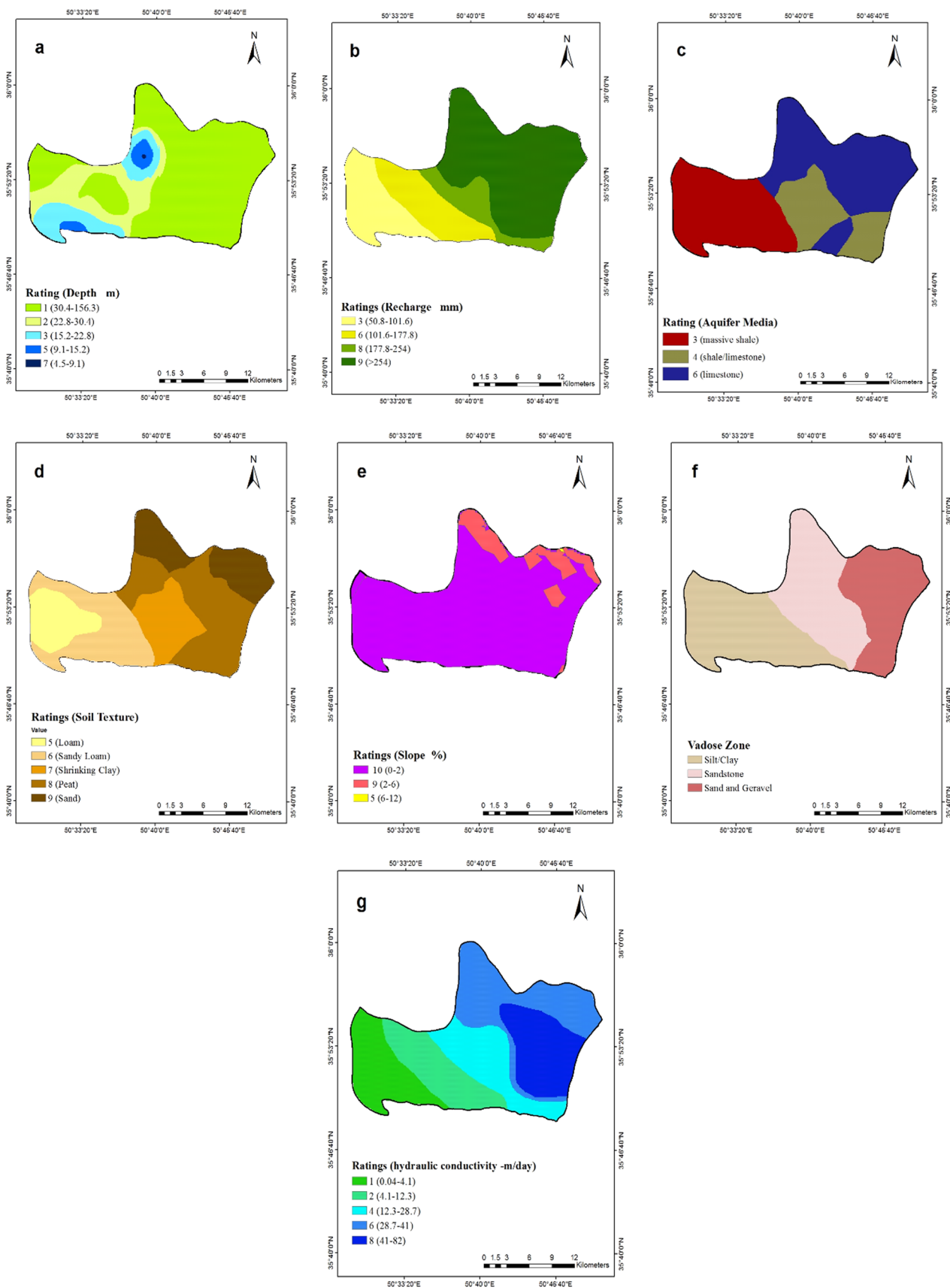


Fig. 5 Maps of the DRASTIC variables

of aquifer recharge (Fig. 5b) was provided based on the information on precipitation, surface runoff, and the water returned to the aquifer. Logging and pumping tests, as well as sampling conducted in the region, were used to record data useful for aquifer media (Fig. 5c), soil media (Fig. 5d), and vadose zone (Fig. 5f) maps. The slope map was prepared according to the digital elevation map (DEM) of the region (Fig. 5e). Finally, the hydraulic conductivity map (Fig. 5g) was obtained from the output of the groundwater modeling after being calibrated in steady-state conditions.

The classifications of all seven variables are shown in Table 2, including relative weights based on Aller et al. (1987). As Fig. 5 depicts, the depth of the water table in the Hashtgerd plain is increased in the west and south areas. The highest rate score associated with the groundwater depth was observed in the southwestern and central regions of the study area, with a water depth between 4.5 and 15.2 m. In addition, the highest recharge (more than 254 mm) was recorded in the northern parts of the aquifer with a rate of 9. Most parts of the study area did not include mountainous topography, with a slope of 0–6%, which has been assigned the DRASTIC rating scores of 9 and 10, indicating their maximum effect on the contamination penetration into the aquifer. The aquifer media, soil media, and vadose zone contained more gravel and sand throughout the study area, so there were three or four classes with rate scores of 4–9.

Since the hydraulic conductivity map was extracted from the groundwater modeling after the calibration stage, it included various values and classes. According to the map

shown in Fig. 3f, the values of hydraulic conductivity varied from more than 40 m per day in the inlet part of the aquifer to less than 4 m per day in the outlet part. Finally, the land use map was classified into five classes using Table 3 (Secunda et al. 1998), the highest (10) and lowest (1) values of which were assigned to the residential and barren and forest areas, respectively.

The DRASTIC vulnerability index was calculated by multiplying the ratings and weights of the variables as introduced in Eq. (1). The resulting map is classified into four classes from low to very high, with the range of 47–154 (Fig. 6a). It reveals that the northeast of the study area has the highest vulnerability with a value of 127–154, while the low vulnerability belongs to the southwest and small parts of the south with a value of 47–74.

By embedding the land use layer to the DRASTIC map, the DRASTIC-Lu map (Fig. 6b) has been obtained. According to the figure, the vulnerability layer has increased by about 30 units with adding the land user layer. So that the value of low vulnerability ranges from 70 to 98, and the value of very high vulnerability is around 153–181. In addition, very high values of vulnerability are concentrated in residential areas of the study region.

MODFLOW simulation

The water table of the aquifer was measured based on the data of 16 observation wells scattered across the area. Then, the groundwater was simulated under steady- and

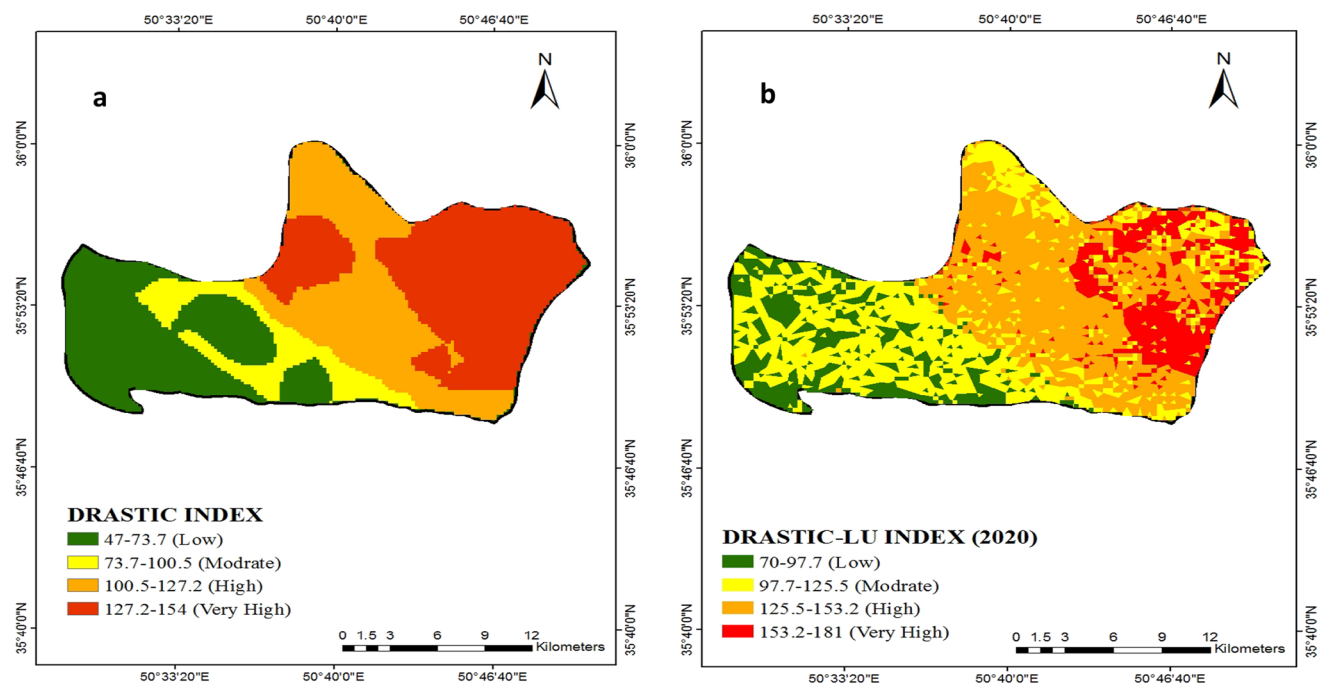


Fig. 6 Resulting maps of the DRASTIC and DRASTIC-Lu indices

unsteady-state conditions. According to the hydrodynamic coefficients of wells and the results of the pumping test, the mean value of specific yield was obtained at 10% throughout the aquifer, where it decreased to 5% in the southeast area and as high as 15% within the area of the Kordan river. Furthermore, according to the water balance report, the mean value of hydraulic conductivity is 20 m per day. Kordan River, flowing from the northeast of the plain toward the southeast, affects hydrological conditions, and hydraulic conductivity might reach 37 m per day in this part of the aquifer (Groundwater Budget Report 2018). The hydraulic conductivity was calibrated using the data from October 2018 for the steady-state conditions and from November 2018–September 2020 for the unsteady-state conditions. First, the initial hydraulic conductivity with an average value of 15 m per day and the specific yield of the aquifer with an average value of 10% entered the model before calibration. Figure 5g depicts hydraulic conductivity values, ranging from 1.8 to 47 m per day. The specific yield, variable between 2 and 20% in various parts of the Hashtgerd aquifer, was calibrated under unsteady-state conditions. RMSE and MAE were calculated to evaluate the model performance under unsteady-state conditions. The maximum error was 0.78 observed in the southern parts of the aquifer, while the minimum error was 0.46 observed in the central regions of the aquifer. The mean RMSE values for the calibration and validation periods were 0.67 and 0.85, respectively, indicating the acceptable performance of the model in simulating the groundwater flow.

After calibration and validation, the maps of groundwater depth and aquifer recharge were obtained from the MODFLOW model to predict DRASTIC in 2030, 2040, and 2050 (Fig. 7). In this regard, the effects of land use changes in the following three periods on the groundwater level and recharge were considered in the model. According to the figure, with increasing the area of agricultural lands and also increasing the irrigation water consumption and the return of agricultural water to the aquifer (return flow), the groundwater depth has changed completely compared to the existing situation, and its level has increased remarkably in some northern and eastern regions. In addition to agricultural use, the increase in residential areas has caused a local rise in groundwater levels in some areas due to the return of effluent water. In addition, due to the overexploitation in the coming years, the water level in some southern and southwestern regions has also decreased. The same trend can be seen in the recharge maps (Fig. 7).

DRASTIC-Lu prediction

After determining the vulnerability map using the DRASTIC-Lu method in the current status as well as the land use maps in 2030, 2040, and 2050, the DRASTIC-Lu prediction

map (DRASTIC-Lu_{pre}) was determined in the future years. Some DRASTIC variables that have a dynamic nature, i.e., recharge and groundwater level, were predicted for the future using the MODFLOW code. By integrating land use maps in the coming years and recharge and groundwater level maps corresponding to land use changes, the DRASTIC-Lu_{pre} map was prepared for the years 2030, 2040, and 2050 (Fig. 8). As can be seen in the figure, there is no significant difference in terms of vulnerability value between DRASTIC-Lu and DRASTIC-Lu_{pre}. The low vulnerability values for all three periods ranged between 70 and 100 for both methods. In addition, the very high vulnerability values were in the range of 150 and 180, especially for 2020, 2040, and 2050. However, there was a significant difference in terms of scattering and level of vulnerability for each class in each period, which is discussed in the following section.

Discussion

Comparison of land use maps

Comparing the current land use map with the future maps in 2030, 2040, and 2050 shows a significant and remarkable difference, especially in agricultural and residential areas. According to Fig. 3, the agricultural area in 2040 and 2050 increased by 250% and 300% compared to the current status, respectively. Of course, this increase will not be significant in the next 10 years, and the agricultural area will increase by 90% in 2030 compared to 2020. In addition, the trend of increasing the residential areas was higher than those of agricultural areas in the coming years, so the residential areas increased by 5 and 8 times in 2040 and 2050 compared to 2020, respectively. The critical point is that, quantitatively, although the changes in urban areas were lower than in agriculture, in terms of the impact on the environment, this increase in residential areas was very significant. Unfortunately, the increase in agricultural and residential areas has greatly reduced the amount of forest and pastures, especially in the period of 2040 and 2050.

Comparison of DRASTIC-Lu and DRASTIC-Lu_{pre} maps

The results showed that adding a land use layer significantly impacted the vulnerability of the Hashtgerd aquifer. Similar results have been reported by Saranya and Saravanan (2021) and Singh et al. (2015). In the latest research conducted in this field by Sarkar and Pal (2021), adding the land use layer in the form of AHP resulted in better performance than the traditional DRASTIC method.

Moreover, regarding the comparison of vulnerability maps in the current status and the future periods, the results showed that the level of vulnerability did not have

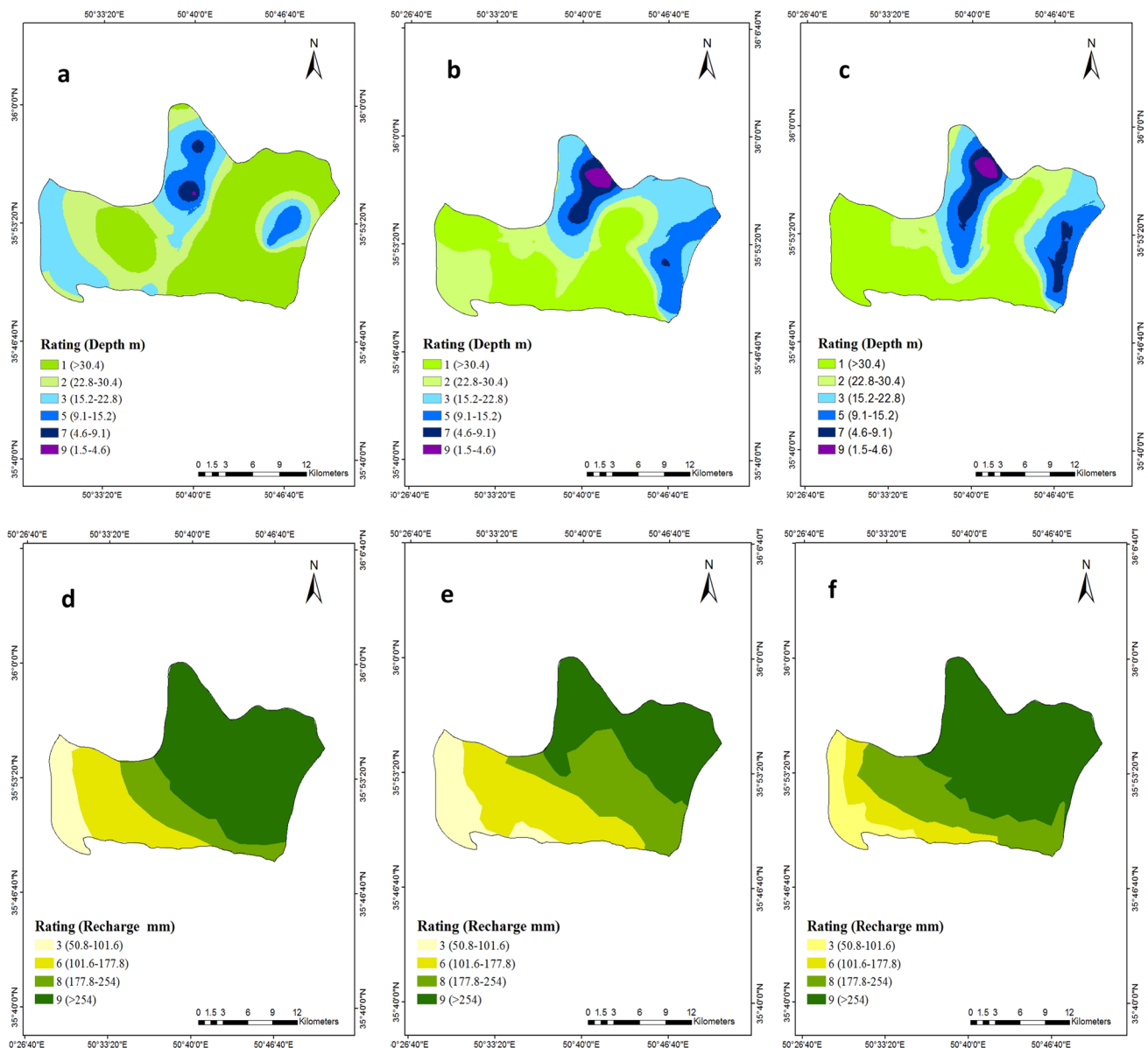


Fig. 7 Predicted maps of groundwater depth and recharge using MODFLOW simulation for 2030, 2040, and 2050

a significant difference in terms of quantity. However, according to Fig. 9, classes with high and very high values of vulnerability had a significant increase in the future compared to the current situation using the DRASTIC- Lu_{pre} , especially with very high values in 2040 and 2050, where an increase of 14% and 50% was observed, respectively, compared to the current situation. This increase is due to noticeable changes in the groundwater level and aquifer recharge in the future, as well as due to the increase in urbanization and agricultural areas. The decrease in the area of pastures and barren lands due to their low ratings has also become an additional cause.

Limitations

This study included several limitations with possibly significant effects on the results. One of its primary limitations was the high uncertainty of land use maps in the future. Although the Kappa coefficient is used to assess the estimations, the prediction of land use changes can involve remarkable errors. This limitation can be solved using the available maps of the past. Moreover, only water consumption changes in agricultural and urban sectors are investigated in preparing the groundwater level and recharge maps in future periods using groundwater modeling according to the future land

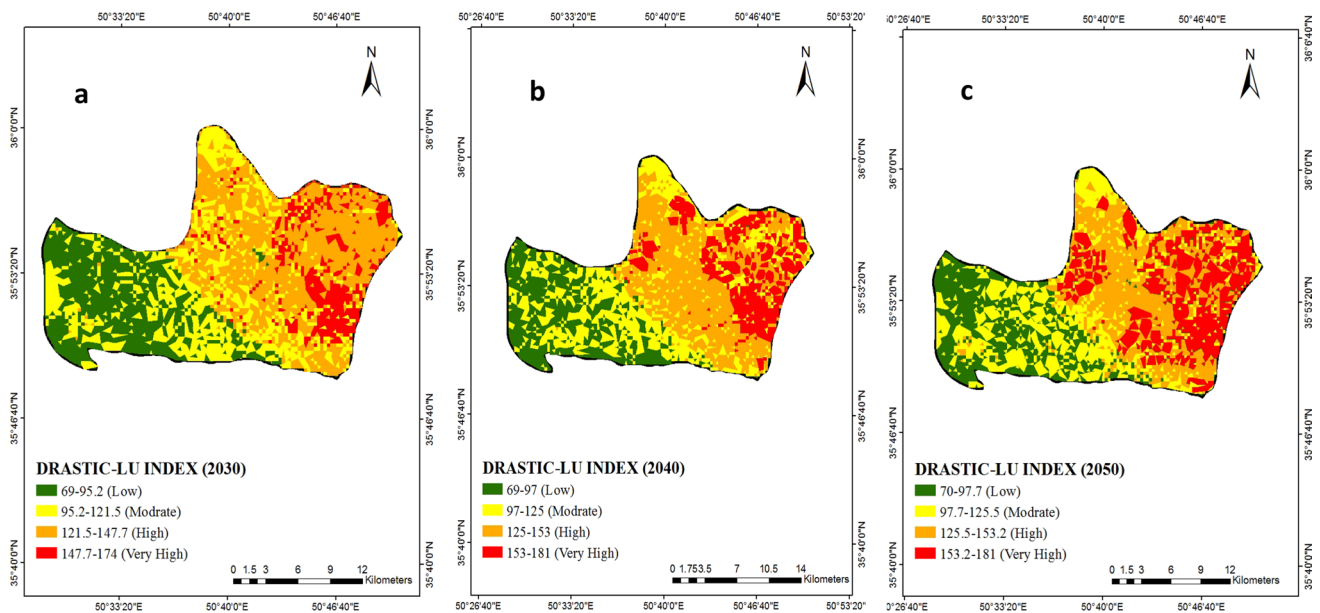


Fig. 8 Resulting maps of the DRASTIC-Lu_{pre} index in 2030, 2040, and 2050

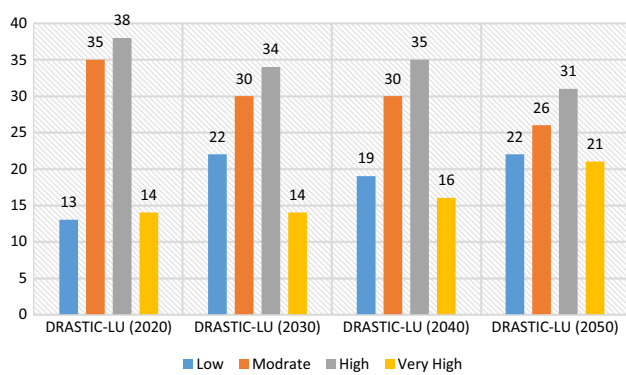


Fig. 9 Resulting maps of the DRASTIC-Lu_{pre} index in 2030, 2040, and 2050

use maps. However, precipitation and climate change can also significantly affect these two maps. This limitation can be addressed significantly using the climate change models of the IPCC sixth report in future research.

Conclusion

Due to the ever-increasing population and urban and rural areas, land use maps will have significant changes in the future. In addition, to improve monitoring and quality management of aquifers in the future, it is necessary to use vulnerability prediction maps. Therefore, this study tried to prepare vulnerability maps for future periods with high accuracy using RS techniques, groundwater modeling, and

land use data. The findings in the first stage showed that land use changes in two classes of residential and agricultural areas increased significantly in 2040 and 2050. These noticeable land use changes will have destructive effects on the environment of the aquifer and its vulnerability. Moreover, the dynamic variables of the DRASTIC method, such as groundwater level and aquifer recharge, suffered from significant changes, and finally, the vulnerability index based on the DRASTIC-Lu_{pre} method changed remarkably compared to the current status. The findings of this study revealed which parts of the aquifer will face a high and very high value of vulnerability in the next 20 and 30 years, making it necessary to adopt quality managerial measures. Finally, the proposed framework makes it possible to know the future vulnerability status of aquifers worldwide, especially those facing remarkable changes in land use.

Supplementary Information The online version contains supplementary material available at <https://doi.org/10.1007/s12665-023-11120-w>.

Author contributions AS: He wrote main manuscript that is included: Conceptualization, Methodology, Software, Validation, Formal analysis; Writing-Original Draft; SJ: Writing-Review & Editing, Formal analysis; Supervision; AH: Formal analysis, Visualization; Investigation; NK: Writing-Review & Editing, RS and GIS analysis, Supervision.

Funding The authors have not disclosed any funding.

Data availability Authors have no restrictions on sharing data.

Declarations

Conflict of interest The authors declare no competing interests.

References

- Abdollahi K, Bashir I, Verbeiren B, Harouna MR, Van Griensven A, Huysmans M, Batelaan O (2017) A distributed monthly water balance model: formulation and application on Black Volta Basin. *Environ Earth Sci* 76(5):198
- Aggarwal S, Gary V, Gupta B, Nikman R, Thakur P (2012) Climate and landuse change scenarios to study impact on hydrological regime. *Int Arch Photogram, Remote Sens Spat Inf Sci* 39:147–152
- Al-Adamat RA, Foster ID, Baban SM (2003) Groundwater vulnerability and risk mapping for the Basaltic aquifer of the Azraq basin of Jordan using GIS, remote sensing and DRASTIC. *Appl Geogr* 23:303–324
- Aller L, Laboratory RSKER (1985) DRASTIC: A standardized system for evaluating ground water pollution potential using hydrogeologic settings. Robert S. Kerr Environmental Research Laboratory, Office of Research and Development, U.S. Environmental Protection Agency
- Aller L, Bennett T, Lehr Jh et al (1987) DRASTIC: a standardized system for evaluating ground water pollution potential using hydrogeologic settings. US Environmental Protection Agency, Washington, DC, p 455
- Allouche J (2016) The birth and spread of IWRM-A case study of global policy diffusion and translation. *Water Alternatives* 9:412
- Almasri MN (2008) Assessment of intrinsic vulnerability to contamination for Gaza coastal aquifer, Palestine. *J Environ Manag* 88:577–593
- Asadi P, Ataie-Ashtiani B, Beheshti A (2017) Vulnerability assessment of urban groundwater resources to nitrate: the case study of Mashhad, Iran. *Environ Earth Sci* 76:1–15
- Balaji L, Saravanan R, Saravanan K, Sreemantharupini NA (2021) Groundwater vulnerability mapping using the modified DRASTIC model: the metaheuristic algorithm approach. *Environ Monit Assess* 193:1–19. <https://doi.org/10.1007/s10661-020-08787-0>
- Birhanu A, Masih I, van der Zaag P et al (2019) Impacts of land use and land cover changes on hydrology of the Gumara catchment, Ethiopia. *Phys Chem Earth, Parts a/b/c* 112:165–174
- Ghosh P, Mukhopadhyay A, Chanda A, Mondal P, Akhand A, Mukherjee S, Nayak SK, Ghosh S, Mitra D, Ghosh T et al (2017) Application of cellular automata and Markov-chain model in geospatial environmental modeling—a review. *Remote Sens Appl Soc Environ* 5:64–77
- Groundwater Budget Report (2018) Basic studies on water resources of Hashtgerd plain. (No. 5–20) Alborz Regional Water Authority. Alborz, Iran
- Hao J, Zhang Y, Jia Y et al (2017) Assessing groundwater vulnerability and its inconsistency with groundwater quality, based on a modified DRASTIC model: a case study in Chaoyang District of Beijing City. *Arab J Geosci* 10:1–16
- Hua A (2017) Application of Ca-Markov model and land use/land cover changes in Malacca River Watershed, Malaysia. *Appl Ecol Environ Res* 15:605–622
- Islam MA (2018) Statistical comparison of satellite-retrieved precipitation products with rain gauge observations over Bangladesh. *Int J Remote Sens* 39:2906–2936
- Javadi S, Kavehkar N, Mousavizadeh MH, Mohammadi K (2011) Modification of DRASTIC model to map groundwater vulnerability to pollution using nitrate measurements in agricultural areas. *JAST* 13:239–249
- Javadi S, Hashemy SM, Mohammadi K et al (2017) Classification of aquifer vulnerability using K-means cluster analysis. *J Hydrol* 549:27–37
- Kardan Moghaddam H, Jafari F, Javadi S (2016) Vulnerability evaluation of a coastal aquifer via GALDIT model and comparison with DRASTIC index using quality parameters. *Hydrol Sci J.* <https://doi.org/10.1080/02626667.2015.1080827>
- Kumar A, Krishna A (2020) Groundwater vulnerability and contamination risk assessment using GIS-based modified DRASTIC-LU model in hard rock aquifer system in India. *Geocarto Int* 35(11):1149–1178
- Machiwal D, Jha MK, Singh VP, Mohan C (2018) Assessment and mapping of groundwater vulnerability to pollution: current status and challenges. *Earth Sci Rev* 185:901–927
- Maghrebi M, Noori R, Bhattarai R et al (2020) Iran's agriculture in the Anthropocene. *Earth's Future.* <https://doi.org/10.1029/2020EF001547>
- Maghrebi M, Noori R, Partani S et al (2021) Iran's groundwater hydrochemistry. *Earth Space Sci.* <https://doi.org/10.1029/2021EA001793>
- Mango L, Melesse A, McClain M, Gann D, Setegn S (2011) Landuse and climate change impacts on hydrology of upper Mara river basin, Kenya: result of modeling study to support better resource management. *Hydrol Earth Syst Sci* 15:2245–2258
- Nadiri AA, Gharekhani M, Khatibi R, Moghaddam AA (2017) Assessment of groundwater vulnerability using supervised committee to combine fuzzy logic models. *Environ Sci Pollut Res* 24:8562–8577. <https://doi.org/10.1007/s11356-017-8489-4>
- Nadiri AA, Moazamnia M, Sadeghfam S et al (2022) Formulating convolutional neural network for mapping total aquifer vulnerability to pollution. *Environ Pollut* 304:119208. <https://doi.org/10.1016/j.envpol.2022.119208>
- Nahin KTK, Basak R, Alam R (2020) Groundwater vulnerability assessment with DRASTIC index method in the salinity-affected southwest coastal region of Bangladesh: a case study in Bagerhat Sadar, Fakirhat and Rampal. *Earth Syst Environ* 4:183–195
- Neshat A, Pradhan B (2017) Evaluation of groundwater vulnerability to pollution using DRASTIC framework and GIS. *Arab J Geosci* 10:501. <https://doi.org/10.1007/s12517-017-3292-6>
- Neshat A, Pradhan B, Pirasteh S, Shafri HZM (2014) Estimating groundwater vulnerability to pollution using a modified DRASTIC model in the Kerman agricultural area, Iran. *Environ Earth Sci* 71:3119–3131. <https://doi.org/10.1007/s12665-013-2690-7>
- Niedertscheider M, Kuemmerle T, Müller D, Erb KH (2014) Exploring the effects of drastic institutional and socio-economic changes on land system dynamics in Germany between 1883 and 2007. *Glob Environ Chang* 28:98–108. <https://doi.org/10.1016/j.gloenvcha.2014.06.006>
- Noori R, Maghrebi M, Mirchi A et al (2021) Anthropogenic depletion of Iran's aquifers. *Proc Natl Acad Sci USA* 118:e2024221118. <https://doi.org/10.1073/pnas.2024221118>
- Pórcel RAD, Schüth C, León-Gómez H, Hoppe A, Lehné R (2014) Land-use impact and nitrate analysis to validate DRASTIC vulnerability maps using a GIS platform of Pablillo River Basin, Linares, NL, Mexico. *Int J Geosci* 5(12):1468–1489. <https://doi.org/10.4236/ijg.2014.512120>
- Purandara BK, Venkatesh B, Jose MK, Chandramohan T (2018) Change of land use/land cover on groundwater recharge in Malaprabha Catchment, Belagavi, Karnataka, India. groundwater. Springer, Singapore, pp 109–120
- Regmi R, Saha S, Balla M (2014) Geospatial analysis of land use land cover change predictive modeling at Phewa Lake Watershed of Nepal. *Int J Curr Eng Tech* 4:2617–2627
- Sahoo M, Sahoo S, Dhar A, Pradhan B (2016) Effectiveness evaluation of objective and subjective weighting methods for aquifer

- vulnerability assessment in urban context. *J Hydrol* 541:1303–1315. <https://doi.org/10.1016/j.jhydrol.2016.08.035>
- Saidi S, Bourri S, Ben Dhia H (2011) Sensitivity analysis in groundwater vulnerability assessment based on GIS in the Mahdia-Ksour Essaf aquifer, Tunisia: a validation study. *Hydrol Sci J-J Des Sci Hydrologiques* 56:288–304
- Salem ZE, Sefelnasr AM, Hasan SS (2019) Assessment of groundwater vulnerability for pollution using DRASTIC Index, young alluvial plain, Western Nile Delta, Egypt. *Arab J Geosci* 12:1–13
- Saranya T, Saravanan S (2021) A comparative analysis on groundwater vulnerability models—fuzzy DRASTIC and fuzzy DRASTIC-L. *Environ Sci Pollut Res*. <https://doi.org/10.1007/s11356-021-16195-1>
- Sarkar M, Pal SC (2021) Application of DRASTIC and modified DRASTIC models for modeling groundwater vulnerability of Malda District in West Bengal. *J Ind Soc Remote Sens* 49, 1201–1219
- Secunda S, Collin ML, Melloul AJ (1998) Groundwater vulnerability assessment using a composite model combining DRASTIC with extensive agricultural land use in Israel's Sharon region. *J Environ Manag* 54(1):39–57
- Singh A, Srivastav SK, Kumar S, Chakrapani GJ (2015) A modified-DRASTIC model (DRASTICA) for assessment of groundwater vulnerability to pollution in an urbanized environment in Lucknow, India. *Environ Earth Sci* 74:5475–5490
- Subedi P, Subedi K, Thapa B (2013) Application of a hybrid cellular automaton-Markov (CA-Markov) Model inland-use change prediction: a case study of saddle creek drainage Basin, Florida. *Appl Ecol Environ Sci* 1:126–132
- Tarawally M, Wenbo X, Weiming H et al (2019) Land use/land cover change evaluation using land change modeller: a comparative analysis between two main cities in Sierra Leone. *Remote Sens Appl: Soc Environ* 16:100262
- Voutchkova DD, Schullehner J, Rasmussen P, Hansen B (2021) A high-resolution nitrate vulnerability assessment of sandy aquifers (DRASTIC-N). *J Environ Manag* 277:111330. <https://doi.org/10.1016/j.jenvman.2020.111330>
- Wang J, He J, Chen H (2012) Assessment of groundwater contamination risk using hazard quantification, a modified DRASTIC model and groundwater value, Beijing Plain, China. *Sci Total Environ* 432:216–226
- Weng Q (2002) Land use change analysis in the Zhujiang Delta of China using satellite remote sensing, GIS and stochastic modeling. *J Environ Manag* 64:273–284
- Yu H, Wu Q, Zeng Y et al (2022) Integrated variable weight model and improved DRASTIC model for groundwater vulnerability assessment in a shallow porous aquifer. *J Hydrol* 608:127538. <https://doi.org/10.1016/j.jhydrol.2022.127538>
- Zhang H, Jiang X-W, Wan L et al (2018) Fractionation of Mg isotopes by clay formation and calcite precipitation in groundwater with long residence times in a sandstone aquifer, Ordos Basin, China. *Geochim Cosmochim Acta* 237:261–274. <https://doi.org/10.1016/j.gca.2018.06.023>

Publisher's Note Springer Nature remains neutral with regard to jurisdictional claims in published maps and institutional affiliations.

Springer Nature or its licensor (e.g. a society or other partner) holds exclusive rights to this article under a publishing agreement with the author(s) or other rightsholder(s); author self-archiving of the accepted manuscript version of this article is solely governed by the terms of such publishing agreement and applicable law.